INDIAN JOURNAL OF SCIENCE AND TECHNOLOGY

RESEARCH ARTICLE

Effect of Deposition Time on the Properties of NiS Films Prepared by Chemical Bath Deposition

K A Jamal Basha[1], Phaneendra Reddy Guddeti[2], Tulasi Ramakrishna Reddy Kotte[1]*

1 Solar Energy Laboratory, Department of Physics, Sri Venkateswara University, Tirupati, 517502, Andra Pradesh, India
2 Faculty in Physics, Department of Humanities and Sciences, Dr. YSR Architecture and Fine Arts University, Kadapa, 516002, Andra Pradesh, India

OPEN ACCESS

Received: 01-09-2022

Accepted: 19-10-2022

Published: 07-12-2022

Citation: Basha KAJ, Guddeti PR, Kotte TRR (2022) Effect of Deposition Time on the Properties of NiS Films Prepared by Chemical Bath Deposition. Indian Journal of Science and Technology 15(45): 2492-2499. https://doi.org/10.17485/IJST/v15i45.1783

* **Corresponding author**.

ktrkreddy@gmail.com

Funding: None

Competing Interests: None

Published By Indian Society for Education and Environment (iSee)

ISSN
Print: 0974-6846
Electronic: 0974-5645

Abstract

Objectives: To study the influence of deposition time on the physical behavior of NiS films formed by chemical bath deposition (CBD). **Methods:** Polycrystalline NiS thin films were deposited by using CBD method on glass substrates by varying the deposition time in the range of 60–150 min with the other growth conditions kept constant. The physical properties were measured using an X-ray diffractometer, Scanning Electron Microscopy with Energy Dispersive X-ray analyzer, and Fourier transform infrared spectra. Finally, the optical and electrical properties of the films were analyzed by using UV-Vis spectrophotometer and linear four-probe point method respectively. **Findings:** The X-ray Diffraction (XRD) studies showed polycrystalline nature of the films with hexagonal structure, confirmed by the Rietveld refinement analysis. The calculated crystallite size varied from 6 nm to 19 nm with the increase in deposition time. The EDS analysis revealed the stoichiometry of Ni and S in the samples. The optical bandgap decreases from 2.06 eV to 1.93 eV with the increase in deposition time. The films synthesized using a deposition time of 120 min at 80 °C showed a high electrical conductivity of 48.3 S/cm at room temperature with activation energy of 0.16 eV. **Novelty**: NiS thin films were deposited by the CBD method using different deposition times varying from 60 min. to 150 min., keeping the bath temperature constant at 80 °C for the first time. The Rietveld refinement analysis was the first of its kind, reported on the structural evaluation of NiS layers. These films were formed using eco-friendly materials adding value to the solar cell application.

Keywords: Thin films; Absorber layer; CBD method; XRD; FTIR

Introduction

In recent years, metal chalcogenide thin films have attracted much attention for photovoltaic energy conversion. Although many metal oxides/hydroxides were

considered for energy conversion, the metal sulphides have been of great interest due to their high electron mobility, better thermal and mechanical stability, unique physical and chemical properties, lower cost, non-toxicity and earth abundancy [1] than metal oxides/hydroxides. The metal sulphides such as copper sulphide (CuS), zinc sulphide (ZnS), cadmium sulphide (CdS), manganese sulphide (MnS), nickel sulphide (NiS), etc. are utilized in different fields such as catalysis, batteries, supercapacitors and solar cells [2–4]. Nickel sulfide (NiS) exhibits high electron conductivity, low-temperature processability, metal-insulating properties, a phase change from paramagnetic to antiferromagnetic and complex phases, which make it a vital transition metal sulfide [5]. NiS exhibits diverse phases with various stoichiometries such as NiS, NiS_2, Ni_3S_2, Ni_3S_4, Ni_6S_5, Ni_7S_6, and Ni_9S_8. Among these phases, it mainly exists in two forms i.e hexagonal (α-NiS), which is stable at high temperatures, and rhombohedral (β-NiS) stable at low temperatures [6]. The hexagonal NiS is known for energy-related applications such as hydrogen evolution reactions, supercapacitors, dye-sensitized solar cells, and lithium-ion batteries [7,8]. Various preparation methods were reported in the literature to deposit NiS such as hydrothermal, microwave synthesis, solvothermal, precipitation, spray pyrolysis, ionic exchange process, screen printing, polyol synthesis, and chemical vapour deposition [9–11]. Among these methods, chemical bath deposition (CBD) is a simple, inexpensive method that does not require sophisticated instruments, minute wastage of precursor materials, and the possibility of film deposition over large surface areas. The literature survey indicated that the reported work on the growth of NiS films by CBD is very meagre. Anuar Kasim et al. deposited NiS films on glass substrates using the CBD method and the influence of triethanolamine on the structural and morphological properties was studied [12]. Sonawane et al. prepared NiS films on glass and stainless steel substrates using the CBD method at room temperature and investigated the electrochemical supercapacitor application [13]. Paresh Gaikar et al. [14] prepared NiS thin films on titanium substrate with additive free by using the chemical bath deposition method for pseudocapacitor application, where the XRD pattern showed polycrystalline nature having a crystalline size of 19 nm. Mohammad Gomma et al., synthesized NiS_2 nanoflake layers on a glass substrate by chemical bath deposition method followed by sulfurization process and reported the crystallite size was 26 nm, and optical properties showed a band gap of 1.19 eV [6]. In CBD, the deposition time is one of the most important factors that affect the release of anions and cations in a reaction bath, which leads to a phase change and variation in grain size along with surface roughness [15]. The variation in deposition time is also one of the key factors in the CBD process to know the optimum condition for the synthesis of the material. To the best of our knowledge, no report has been published on the effect of deposition time on the properties of NiS thin films, deposited by the CBD method. In the present work, NiS thin films were deposited by using CBD process at various deposition times such as 60 min, 90 min, 120 min, and 150 min. while the bath temperature remains constant at 80 °C. The structural, compositional, optical, and electrical properties of deposited NiS films were investigated and analyzed. In particular, the structural analysis was made using Rietveld refinement analysis to evaluate the crystal structure of the grown films.

Methodology

2.1 Preparation of NiS films

Polycrystalline NiS thin films were deposited by using CBD method on soda lime glass substrates. The preparation involves 20 ml 0.8 M nickel sulphate hexahydrate ($NiSO_46H_2O$) as Ni source with purity of 99.9%, 20 ml of 0.8 M thioacetamide (C_2H_5NS) as S source with 99.99% purity, 4 ml Triethanolamine [$N(CH_2CH_2OH)_3$], 5 ml ammonia (NH_3) and 20ml deionized water so that the total volume of reaction bath was 100 ml. The pH of the solution was maintained at 9.5. Among these constituents, triethanolamine was used as a complexing agent, and NH_3 to control the pH value of the solution. NiS films were prepared on glass substrates using different deposition times, 60 min, 90 min, 120 min, and 150 min respectively, at a constant bath temperature of 80 °C.

2.2 Characterization

The crystallinity and other structural parameters of NiS films were investigated by using a Rigaku X-ray diffractometer (Miniflex600). The surface morphology and compositional analysis were carried out by JEOLJSM-IT500 Scanning Electron Microscopy, attached with the AMETEK make Energy Dispersive X-ray analyzer. A BRUKER FT-IR spectrometer was used to record the Fourier transform infrared spectra in the wave number range, 500-4000 cm^{-1} to identify the functional groups present. The thickness is measured by using stylus thickness profile meter. The optical properties of the films were analyzed by using SHIMADZU (UV-2600i model) UV-Vis spectrophotometer. The electrical parameters were measured by using the linear four-probe point method.

Results and discussion

3.1 Structural properties

The deposited films appeared black in color and pinhole free. The scratch tape test revealed that the layers were strongly adherent to the substrate surface.

Figure 1 (a) shows the X-ray diffractograms of NiS films deposited at different deposition times varied from 60 min to 150 min, while keeping the temperature constant at 80 °C. The figure reveals that the deposited films were polycrystalline with hexagonal structure and the main peak is strongly oriented along the (010) plane. The XRD spectra indicate four peaks appeared at 2θ= 30.92°, 35.43°, 46.50° and 54.37°, which corresponds respectively to the (010), (011), (012) and (110) planes of NiS. This indicates that the deposited films had a single phase. The observed peak positions are in good agreement with the standard JCPDS card (01-075-0613). NiS films obtained at deposition times 60 min and 90 min showed small peaks with low intensities with a slightly amorphous background. As the deposition time increases from 90 min to 120 min, the film structure turns into crystalline nature, and the intensity of peaks increases due to atomic condensation during the film formation. Further increase of deposition time to 150 min. decreases the peak intensity. This is probably because of the disintegration of the crystallites thereby decreasing the crystallinity and intensities of the peaks. The average crystalline size was calculated from the full-width at half maximum (FWHM) of the XRD peaks by using the Scherer formula:

$$D = \frac{0.9\lambda}{\beta \cos\theta} nm \tag{1}$$

where λ is the X-ray wavelength (λ=1.5406A°), β is the observed angular width at half maximum intensity (FWHM) of the peak and θ is the Bragg angle. The average grain size evaluated for the (100) plane is 19 nm at the deposition time of 120 min, which decreases to 12 nm at 150 min. deposition time. The decrease in crystallite size may be due to Vander Waals forces which decrease the mutual attraction between the crystallites, as the films remain in solution longer deposition times than required.

The crystallite size, bond length, positional parameter, dislocation density, and micro strain of NiS films deposited at 90 min., 120 min, and 150 min were calculated using the following equations [16] and the calculated values are listed in Table 1. The unit cell parameters a, b, and c of hexagonal NiS were calculated through the following equation.

$$\frac{1}{d^2} = \frac{4\left(h^2 + hk + k^2\right)}{3a^2} + \frac{l^2}{c^2} \tag{2}$$

where, d_{hkl} is the inter-planar spacing; a and c are the lattice parameters; h, k, and l are the miller indices.

The microstrain

$$\varepsilon = \frac{\beta}{4\tan\theta} \tag{3}$$

The dislocation density

$$\delta = \frac{1}{D^2} \text{ Lines } /\text{m}^2 \tag{4}$$

The positional parameter

$$u = \frac{a^2}{3c^2} + 0.25 \tag{5}$$

The bond length

$$l = \sqrt{\frac{a^2}{3} + \left(\frac{1}{2} - u\right)^2 c^2} \tag{6}$$

The volume (V) of the unit cell

$$V = 0.86 \times a^2 \times c \tag{7}$$

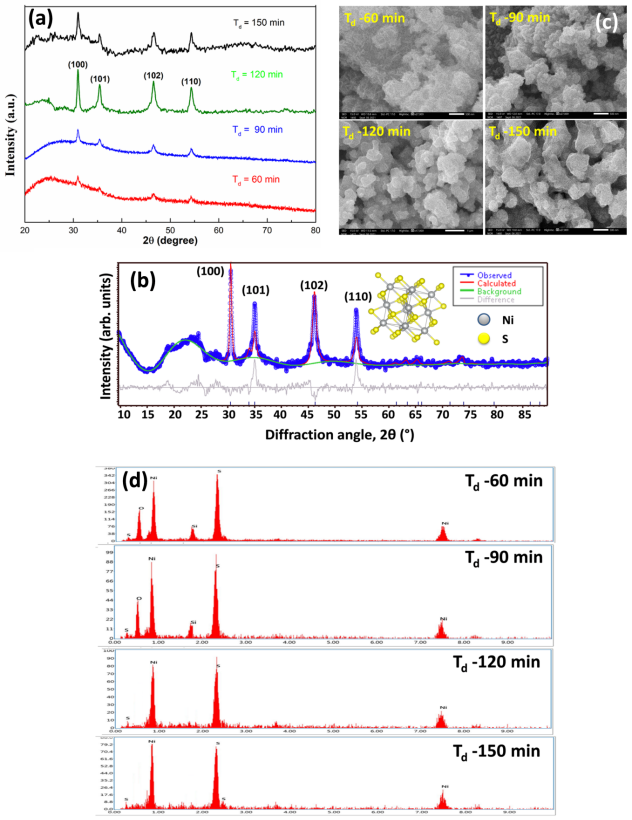

Fig 1. (a) X-ray diffraction pattern of the NiS thin films for various deposition times from 60 min to 150 min. **(b)** Rietveld-refinement profile of XRD data of NiS film deposited at 120 min deposition time. **(c)** The SEM images **(d)** EDS spectra of NiS films prepared at the various deposition times at constant temperature 80 $^{\circ}$C

Table 1. Average grain size, bond length, Positional parameter, dislocation density and micro strain of the NiS thin films at different deposition times

Deposition Time (min)	Crystallite size (nm)	Bond length (l) (A^o)	Positional parameter (u)	Dislocation density (x10^{15}) Lines /m^2	Micro strain (10^{-3})
90	07	2.06	0.386	2.0	2.7
120	19	2.07	0.388	2.8	4.1
150	11	2.07	0.391	8.3	6.5

Figure 1 (b) shows Rietveld refinement of XRD diffractograms of NiS thin films formed at 120 min. The analysis of Rietveld refinement was also done to know the crystalline structure and lattice parameters of 120 min. deposited NiS thin film. In addition, R weighted profile (Rwp), R profile (Rp), R structure factor, R Bragg factor (R_{Bragg}), and goodness of fit (GOF) such structural parameters were also calculated. EXPO software was used to calculate the unit cell parameters from the Rietveld refinement data. The calculated Rietveld refinement parameters such as R_p, R_{wp}, GOF, R structure factor, R_{Bragg}, and unit cell parameters were listed in Table 2. As the GOF value is 8.01, one can speak about the quality of the goodness of refinement of as-prepared thin films.

Table 2 shows the site occupancies of Ni and S atoms distributed along fractional coordinates. It contains one nickel site (Ni) and one sulphur site (S). Further, the crystal structure and atomic bonding in NiS film were evaluated from Veesta software. It indicates that the deposited NiS film exhibited a hexagonal crystal structure with the space group P 63/ m m c (space group number: 194). The NiS film prepared at a deposition time of 120 min contains 44 atoms that are distributed in the hexagonal structure with 72 bonds. The structure parameters are already listed in Table 2, and the related crystal structure is also shown

in the inset of Figure 2.

Table 2. Calculated lattice structure and refinement parameters from Rietveld refinement pattern for NiS thin films at deposition time 120 min

Unit cell parameters	
a, (Å)	3.421
b, (Å)	3.421
c, (Å)	5.339
α,(°)	90
β, (°)	90
γ, (°)	120
Cell volume (Å)^3	54.1123
Density (g/cm^3)	5.61
Crystal system & Space group number	Hexagonal& (P 63/m m c)
Structure parameters	
Atoms	44
Bonds	72
Polyhedra	12
Refinement parameters	
R_p	10.515
R_{wp}	13.767
Goodness of fit (GOF)	8.01
R-Structure factor	13.520
R-Bragg factor	17.960
Site occupancies	
Ni	**X** = 0.00000, **Y** = 0.00000, **Z** = 0.000, **Occupancy**: 1.0000, **U**=0.006, **Site**: 2a, **Sym.**: -3m
S	**X** = 0. 33333, **Y** = 0.66667, **Z** = 0.25000, **Occupancy**:1.0000, **U** = 0.006, **Site**: 2c, **Sym.**: -6m2

3.2 Morphological properties

The surface morphology of NiS films prepared at different deposition times was characterized by SEM images, shown in Figure 1 (c). From the SEM images, a change in the morphology of NiS was observed with the increase in deposition time. At a lower deposition time of 60 min. densely aggregated larger lumps were observed, which might be due to poor nucleation and growth rate. As the deposition time increased to 90 min., aggregation of grains increased leading to flower-like morphology. For a reaction time of 120 min., bigger grains with uniform, homogeneous and hexagonal-like morphology were observed. This might be due to more adsorption of NiS on the substrate. As the deposition time was increased to 150 min, the intergrain boundaries overlapped due to cluster growth and disassociation of grains because of a decrease in van der Wall forces, leading to the formation of more voids in the film. From SEM analysis it can be concluded that 120 min deposition time is optimum for the growth of films that had uniform and homogeneous grains distributed on the surface.

3.3 Composition analysis

Figure 1 (d) reveals an elemental compositional analysis of the NiS thin films, measured using EDS. The EDS study confirms the existence of both Ni and S with various stoichiometries. The atomic weight % of Ni, S, and ratio of Ni/S for films formed at different deposition times are listed in Table 3. The presence of Si and O in addition to Ni and S was observed for the deposition time of 60 and 90 min, which might be from the glass substrate as the film thickness might be less for such low deposition times. The atomic weight % of Ni and S was increased with the increase of the deposition time. It confirms the impact of deposition time on atomic weight % and composition of the prepared NiS films. For the deposition time up to 120 min, the Ni/S atomic ratio was nearly close to unity. The atomic weight % of sulphur decreased for the longer deposition time (150 min).

3.4 FTIR Analysis

Fourier Transform Infrared Spectroscopy study is carried out to identify and analyze the different functional groups present in the prepared NiS films over the wave number range between 500 cm^{-1} and 4000 cm^{-1} (see Figure 2 (a)) The weak bands or shoulders observed at 713, 826 and 903 cm^{-1} were related to the symmetrical stretching modes of NiS, which could be due to microstructural formation of NiS in the films and are in agreement with the data reported in the literature [17]. The band at 1523 and 1685 cm^{-1} corresponds to -COOH asymmetric stretching vibration. Non-appearance of other modes in the wave number range, 2500 - 2600 cm^{-1} indicates the absence of S-H stretching mode in the films. The peaks noticed at the wave numbers 3616 cm^{-1}, 3734 cm^{-1}, and 3853 cm^{-1} are related to the stretching modes of the O-H group.

3.5 Optical studies

Figure 2 (b) shows the optical transmittance versus wavelength spectra of NiS thin films prepared using different deposition times. From the fig, it is observed that all the films exhibited similar transmittance patterns, and the transmittance increases with the increase of deposition time. All the films showed a sudden fall in the transmittance near the fundamental absorption edge, indicating the presence of direct optical transition in the films. The slight decrease of transmittance for the films formed at 150 min might be due to a change in the crystallinity of the films.

Using the transmittance data, the absorption coefficient was calculated by using the following formula,

$$\ln T = -\alpha t \tag{8}$$

where T is the optical transmittance, α is the absorption coefficient and t is the film thickness. In the present work, the film thickness is taken as 160 nm, 205 nm, 243 nm, and 285 nm for the films prepared using deposition times of 60 min, 90 min, 120 min, and 150 min respectively. Figure 2 (c) represents the band gap values of the NiS films prepared by the CBD method. The optical band gap of as-prepared NiS films at various deposition times was calculated by using the following relation.

$$\alpha h\upsilon = B\left(h\upsilon - E_g\right)^n \tag{9}$$

where α is the absorption coefficient, B is a constant, and n indicates the type of band gap (n = 1/2 for direct allowed transition and n = 2 indirect allowed transition). The straight lines drawn from the linear portion of the $(\alpha h\upsilon)^2$ vs $h\upsilon$ curves onto the X-axis give the value of the energy band gap in the films. From Figure 2 (c) the calculated band gap energies were 2.06 eV,1.97 eV, and 1.93 eV for NiS films formed using deposition times 60 min, 90 min, and 120 min respectively. Quantum size effect, variation in barrier height, lattice constants, and impurities are the diverse factors that affect the band gap energy in thin films. As the deposition time was increased from 60 to 120 min., the band gap energy decreased from 2.06 eV to 1.93 eV. The decrement in band gap can be attributed to an increase in grain size with an increase in deposition time. Further increase in deposition time to 150 min increases the band gap to 2.09 eV. This is because of the decrease in grain size at such deposition times, as observed in the structural properties, which might result in the splitting of energy levels between valence and conduction bands leading to an increase in band gap at longer deposition time [18]. The obtained energy gap values were slightly lower than the bulk NiS [19].

3.6 Electrical properties

The electrical properties of the prepared NiS films were measured using linear four-probe point method at room temperature.Table 4 gives the measured electrical properties of the grown NiS thin films. From Table 4, it can be seen that the films have high electrical conductivity of 48.3 S/cm, which might be due to the better crystallinity and stoichiometry of these layers. The resistivity of NiS thin films decreased with increase in deposition time of up to 120 min. This might be due to the improvement in crystallinity which leads to less scattering of carriers at grain boundaries. Due to the overlapping of grain boundaries, the resistivity of the film increases at a longer deposition time of 150 min.

The change of electrical conductivity with temperature followed the Arrhenius relation denoted in Eq (10).

$$\sigma = \sigma_0 e^{-E_a/KT} \tag{10}$$

where σ is conductivity at temperature T,σ_0 is a constant, k is a Boltzmann constant, E_a is activation energy and T is the absolute temperature. The variation of log (s) with inverse temperature (1000/T) for NiS films is shown in Figure 2 (d). The straight-line nature in the graph in Figure 2 (d) indicates the semiconducting behavior of the film. The activation energy of films was calculated from the linear fit of the log (s) versus temperature (1000/T) curve and found to be 0.16 eV for the film deposited at 120 min deposition time. This value is in close agreement with the value reported by Kumar et al. [20] for NiS thin films grown by the screen printing method.

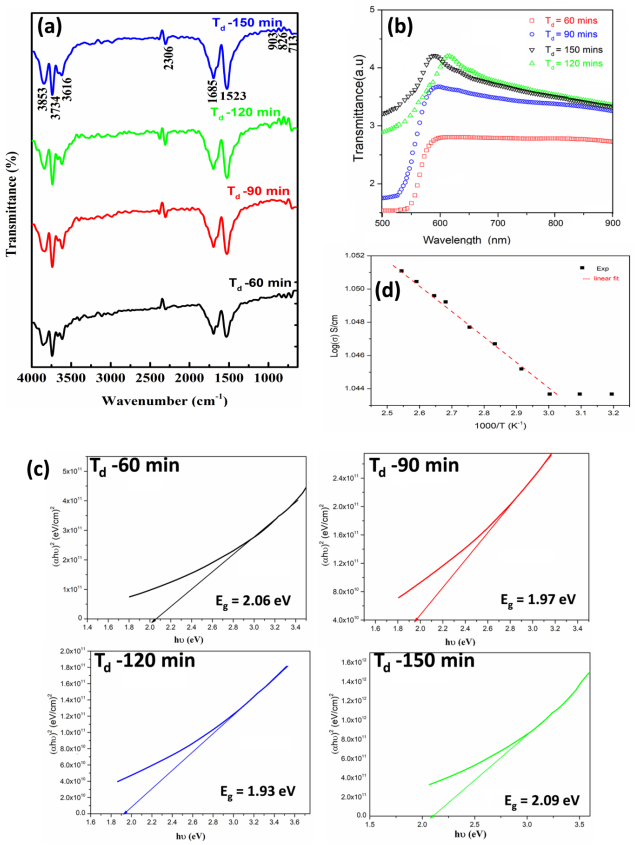

Fig 2. (a) FTIR spectra of NiS films prepared with different deposition times. **(b)** UV-Vis transmittance spectra of NiS films. **(c)** Plots of $(\alpha h\upsilon)^2$ versus photon energy ($h\upsilon$) of NiS films prepared at deposition time of a) 60, b) 90, c) 120, and d)150 min. **(d)** The plot of log (conductivity) versus 1000/T of chemical bath deposited NiS film at deposition time of 120 min

Table 3. Atomic % of Ni and S thin films

Deposition time (min)	Ni (at. %)	S (at. %)	Si at. %	O at. %	Ni/S ratio
60	32.68	31.68	17.76	17.88	1.03
90	42.30	39.94	5.75	12.01	1.05
120	52.15	47.85	—	—	1.08
150	53.25	46.75	—	—	1.13

Table 4. The electrical parameters of CBD films

Deposition time (min)	Thickness (nm)	Electrical Resistivityρ $(\Omega.cm)^{-1}$	Electrical Conductivity σ (S/cm)
60	160	7.43×10^{-1}	1.35
90	205	6.62×10^{-1}	1.51
120	243	2.07×10^{-2}	48.3
150	285	4.31×10^{-2}	23.2

Conclusions

NiS films were successfully deposited on glass substrates by using the chemical bath deposition method at a bath temperature of 80 °C. The influence of deposition time varies in the range of 60-150 min. on the physical properties was investigated for the first time. The XRD data revealed the polycrystalline nature of the films with the hexagonal structure. The Rietveld refinement analysis confirmed the hexagonal structure of the deposited films. Optical band gap values for all the deposited films varied in the range of 1.93 - 2.09 eV. The film deposited using 120 min., had a maximum crystallite size of 19 nm and showed near stoichiometric composition of Ni and S. The films deposited using a time of 120 min. showed the highest electrical conductivity of 48.3 S/cm with activation energy of 0.16 eV. Such highly conducting, large band gap, and good crystalline films may be useful as an absorber layer for solar cell applications.

References

1) Liu R, Zhou A, Zhang X, Mu J, Che H, Wang Y, et al. Fundamentals, advances and challenges of transition metal compounds-based supercapacitors. *Chemical Engineering Journal*. 2021;412:128611. Available from: https://doi.org/10.1016/j.cej.2021.128611.
2) Li W, He X, Xin K, He X, Lin H, Qin L, et al. *bio template synthesis of zinc sulfide spheres with high photocatalytic performance on organic dyes journal of materials engineering and performance*. 2020;29:4569–4574. Available from: https://doi.org/10.1007/s11665-020-04966-9.
3) Sahu R, Patodia T, Yadav D, Jain SK, Tripathi B. Visible-light induced photo catalytic response of MWCNTs-CdS composites via efficient interfacial charge transfer. *Materials Letters: X*. 2022;13:100116. Available from: https://doi.org/10.1016/j.mlblux.2021.100116.
4) Pallavolu MR, Reddy VRM, Guddeti PR, Park C. Development of SnSe thin films through selenization of sputtered Sn-metal films. *Journal of Materials Science: Materials in Electronics*. 2019;30:15980–15988. Available from: https://doi.org/10.1007/s10854-019-01968-9.
5) Shombe MDGB, Khan C, Zequine C, Zhao RK, Gupta. Direct solvent free synthesis of bare α-NiS, β-NiS and α-βNiS composite as excellent electrocatalysts: Effect of self capping on super capacitance and overall water splitting activity. *Nature Scientific Reports* . 2019;10. Available from: https://doi.org/10.1038/s41598-020-59714-9.
6) Gomaa MM, Sayed MH, Abdel-Wahed MS, Boshta M. A facile chemical synthesis of nanoflake NiS₂ layers and their photocatalytic activity. *RSC Advances*. 2022;12:10401–10408. Available from: https://doi:10.1039/D2RA01067D.
7) Cao X, Ding R, Zhang Y, Cui Y, Hong K. A heterojunction film of NiS2 and MnS as an efficient counter electrode for dye-sensitized solar cells. *Materials Today Communications*. 2021;26:102160. Available from: https://doi.org/10.1016/j.mtcomm.2021.102160.
8) Song K, Li W, Yang R, Zheng Y, Chen X, Wang X, et al. Controlled preparation of Ni(OH)2/NiS nanosheet heterostructure as hybrid supercapacitor electrodes for high electrochemical performance. *Electrochimica Acta*. 2021;388:138663. Available from: https://doi.org/10.1016/j.electacta.2021.138663.
9) Salleh SA, Rahman MYA, Aziz THT. Dye-sensitized solar cell using nickel sulfide-reduced graphene oxide counter electrode: Effect of sulphur content. *Inorganic Chemistry Communications*. 2022;135:109086. Available from: https://doi.org/10.1016/j.inoche.2021.109086.
10) Patel PC, Mishra PK, Kandpal HC. Low temperature magnetic study of α-NiS nanoparticles synthesized via hydrothermal technique. *Materials Today: Proceedings*. 2021;47(8):1550–1556. Available from: https://doi.org/10.1016/j.matpr.2021.03.499.
11) Suganya G, Kalpana G. Investigation of graphene based NiS nanocomposite by solvothermal method for energy storage application. *Materials Letters: X*. 2021;12:100112. Available from: https://doi.org/10.1016/j.mlblux.2021.100112.
12) Kassim. Influence of Triethanolamine on the Chemical Bath Deposited NiS Thin Films. *American Journal of Applied Sciences*. 2011;8(4):359–361. Available from: https://doi.org/10.3844/ajassp.2011.359.361.
13) Sonawane MS, Patil AM, Patil RS. Synthesis and Characterization of Chemically Deposited Nickel Sulphide Thin Film Electrodes for Electrochemical Supercapacitor Application. *Volume 5, Issue 4*. 2019;5(4):761–764. Available from: https://doi.org/10.30799/jnst.243.19050405.
14) Gaikar P, Pawar SP, Mane RS, Nuashad MU, Shinde DV. Synthesis of nickel sulfide as a promising electrode material for pseudocapacitor application. *RSC Advances*. 2016;6(113):112589–112593. Available from: https://doi:10.1039/C6RA22606J.
15) Zafar S, Iqbal MA, Malik M, Shahid W, Irfan S, Shabir MY, et al. Surface Morphology, Roughness, and Structural Characteristics of Al1−xMgxSb (x = 0 and 0.1) Thin Films Deposited by Chemical Bath Deposition Technique. *Applied Sciences*. 2022;12(15):7412. Available from: https://doi.org/10.3390/app12157412.
16) Iram S, Mahmood A, Ehsan MF, Mumtaz A, Sohail M, Sitara E, et al. Impedance Spectroscopic Study of Nickel Sulfide Nanostructures Deposited by Aerosol Assisted Chemical Vapor Deposition Technique. *Nanomaterials*. 2021;11(5):1105. Available from: https://doi.org/10.3390/nano11051105.
17) Gahtar A, Benramache S, Ammari A, Boukhachem A, Ziouche A. Effect of molar concentration on the physical properties of NiS thin film prepared by spray pyrolysis method for supercapacitors. *Inorganic and Nano-Metal Chemistry*. 2022;52(1):1–10. Available from: https://doi:10.1080/24701556.2020.1862225.
18) Kotei PA, Boadi NO, Saah SA, Mensah MB. Synthesis of Nickel Sulfide Thin Films and Nanocrystals from the Nickel Ethyl Xanthate Complex. *Advances in Materials Science and Engineering*. 2022;2022:1–10. Available from: https://doi.org/10.1155/2022/6587934.
19) Kristl M, Dojer B, Gyergyek S, Kristl J. Synthesis of nickel and cobalt sulfide nanoparticles using a low cost sonochemical method. *Heliyon*. 2017;3(3):e00273. Available from: https://doi.org/10.1016/j.heliyon.2017.e00273.
20) Kumar V, Sharma DK, Sharma KK, Dwivedi DK. Investigation on physical properties of polycrystalline nickel sulphide films grown by simple & economical screen-printing method. *Optik*. 2018;156:43–48. Available from: https://doi.org/10.1016/j.ijleo.2017.10.169.